Supporting Information

The impact of the cation alkyl chain length on the wettability of alkylimidazolium-based ionic liquids at the nanoscale

José C. S. Costa,* Alexandre Alves, Margarida Bastos, Luís M. N. B. F. Santos

CIQUP, Institute of Molecular Sciences (IMS), Department of Chemistry and Biochemistry, Faculty of Science, University of Porto, Rua do Campo Alegre, P4169 007 Porto, Portugal
**E-mail: jose.costa@fc.up.pt*

Index

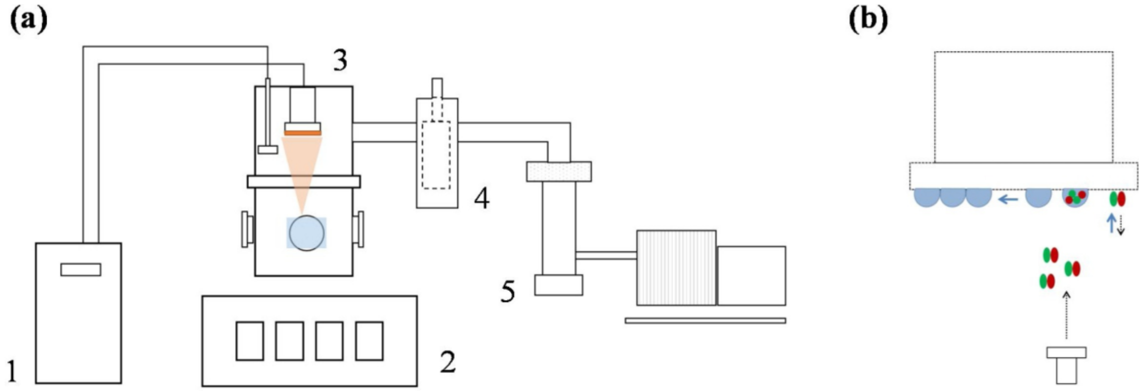

Fig. S1. Schematic representation of the physical vapor deposition methodology: (a) ThinFilmVD apparatus (1 – cooling system, 2 – instrumentation box, 3 – vacuum chamber, 4 – N_2 (l) metallic trap, 5 – vacuum pumping system); (b) schematic detail of the PVD of ionic liquids. More details: *Appl. Surf. Sci.*, 2018, 428, 242 and *J. Chem. Eng. Data*, 2015, 60, 3776.

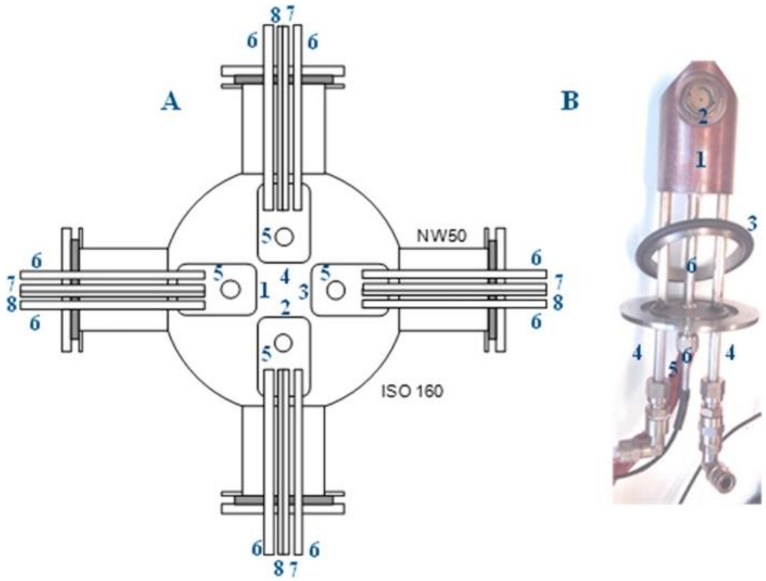

Fig. S2. A – Schematic representation of the ovens: 1, 2, 3, 4 – individual ovens; 5 – cavity of the Knudsen cell screwing; 6 – air cooling tube; 7 – heater; 8, – Pt100 sensor; B – Image of an individual oven (top view): 1 – copper block; 2 – Knudsen cell; 3 – Viton O-ring; 4 – cooling system; 5 – heater; 6 – Pt100. More details: *J. Chem. Eng. Data*, 2015, 60, 3776.

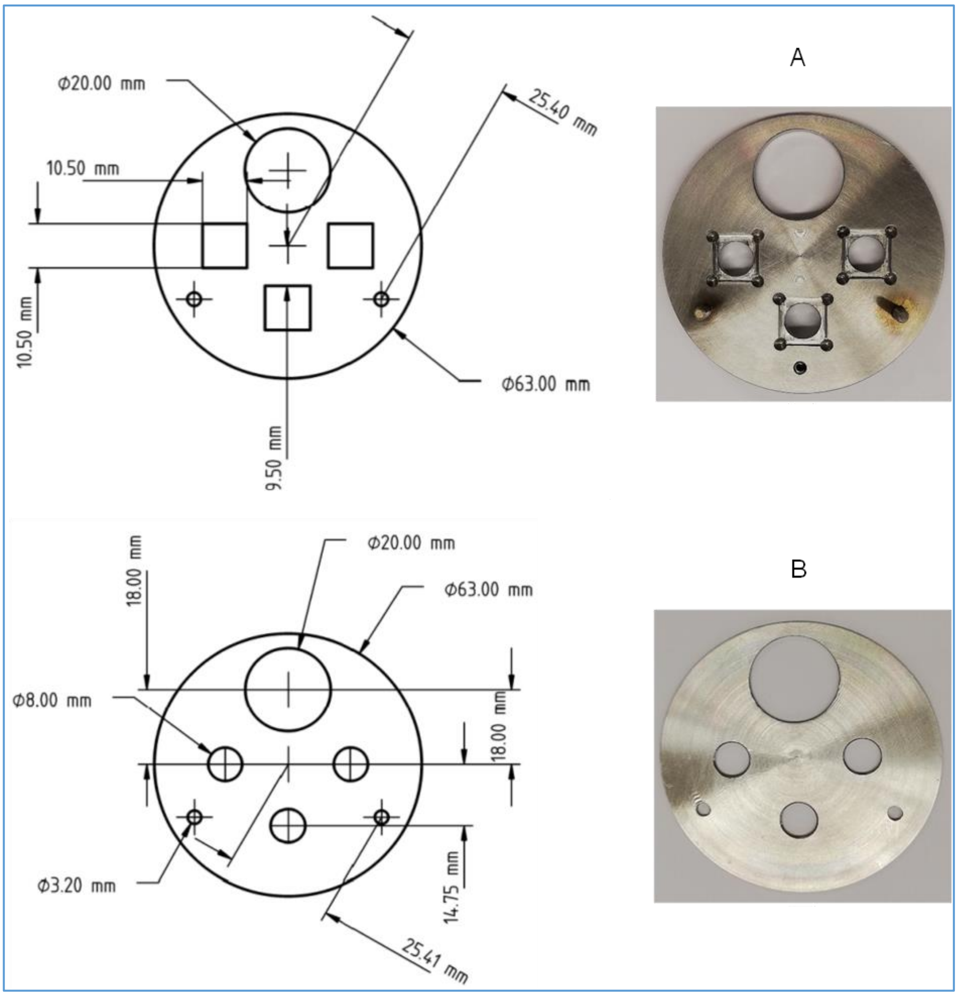

Fig. S3. A – Schematic representation (left) and images (right) of the substrate support system. The support was used for the simultaneous deposition of each IL on three different surfaces: ITO/glass; Ag/ITO/glass; Au/ITO/glass.

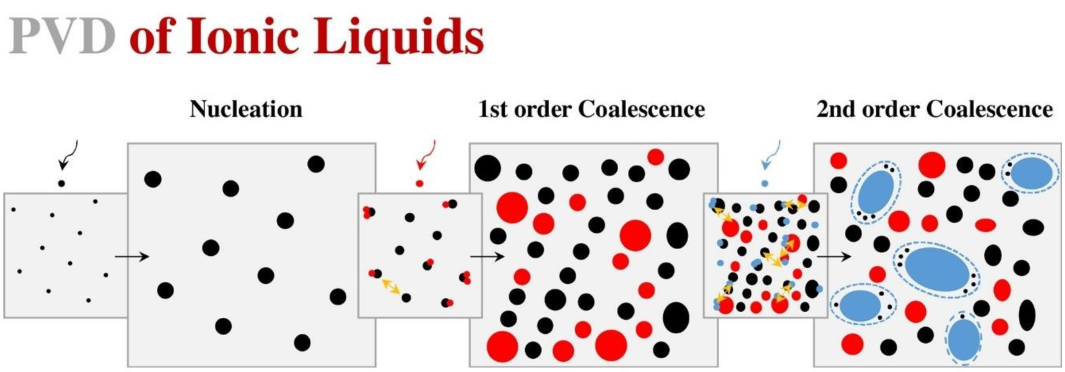

Fig. S4. Mechanisms of nucleation and growth of ionic liquid films: minimum free area to promote nucleation (MFAN); first-order coalescence; second-order coalescence. More details: *Appl. Surf. Sci.*, 2018, 428, 242.

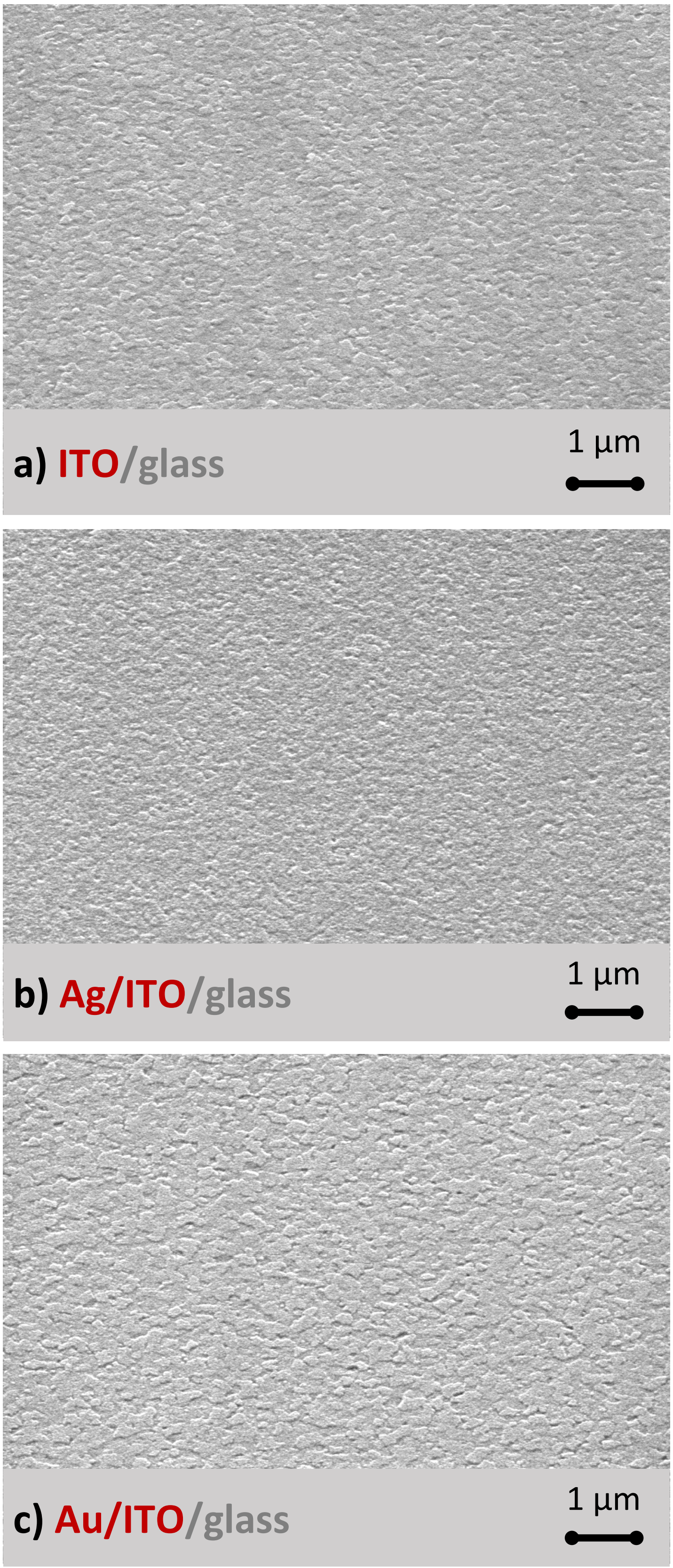

Fig. S5. Morphology of the substrates: indium tin oxide (ITO)/glass surface (a); silver(Ag)/ITO/glass surface (b); gold(Au)/ITO/glass surface. Micrographs were acquired through high-resolution scanning electron microscopy (SEM) by using a secondary electron detector (SED). Lateral views at 45° were obtained with a magnification of 25000×.

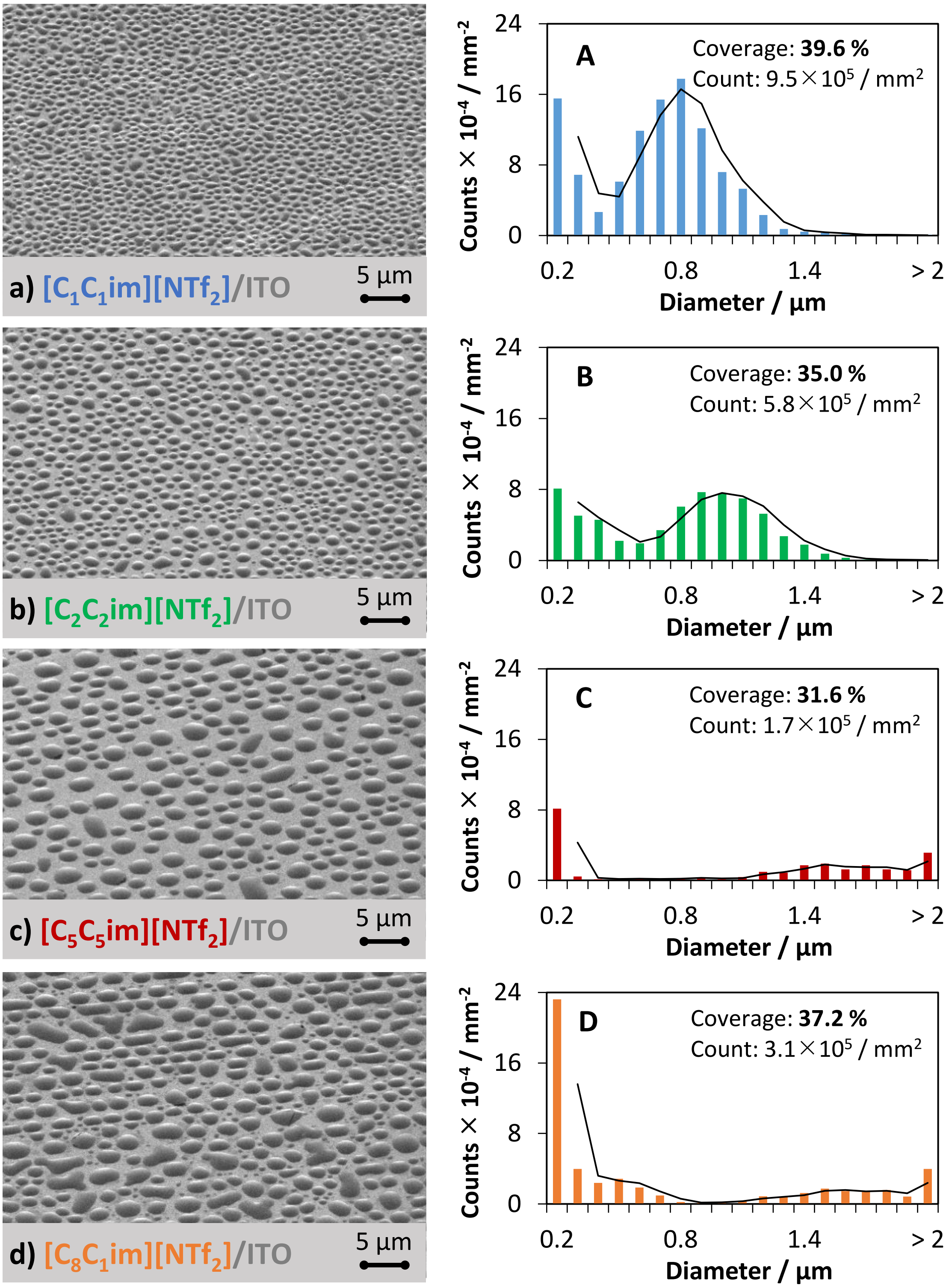

Fig. S6. Morphology of vapor-deposited ionic liquids (50 monolayers) onto indium tin oxide (ITO)/glass surfaces (a, b, c, d) and the respective droplet size distribution (A, B, C, D): $[C_1C_1im][NTf_2]$ (a, A), $[C_2C_2im][NTf_2]$ (b, B), $[C_5C_5im][NTf_2]$ (c, C), and $[C_8C_1im][NTf_2]$ (d, D). The ionic liquids were deposited under the same experimental procedure and setup. Micrographs were acquired through high-resolution scanning electron microscopy (SEM) by using a secondary electron detector (SED). Lateral views at 45° were obtained with a magnification of 5000×.

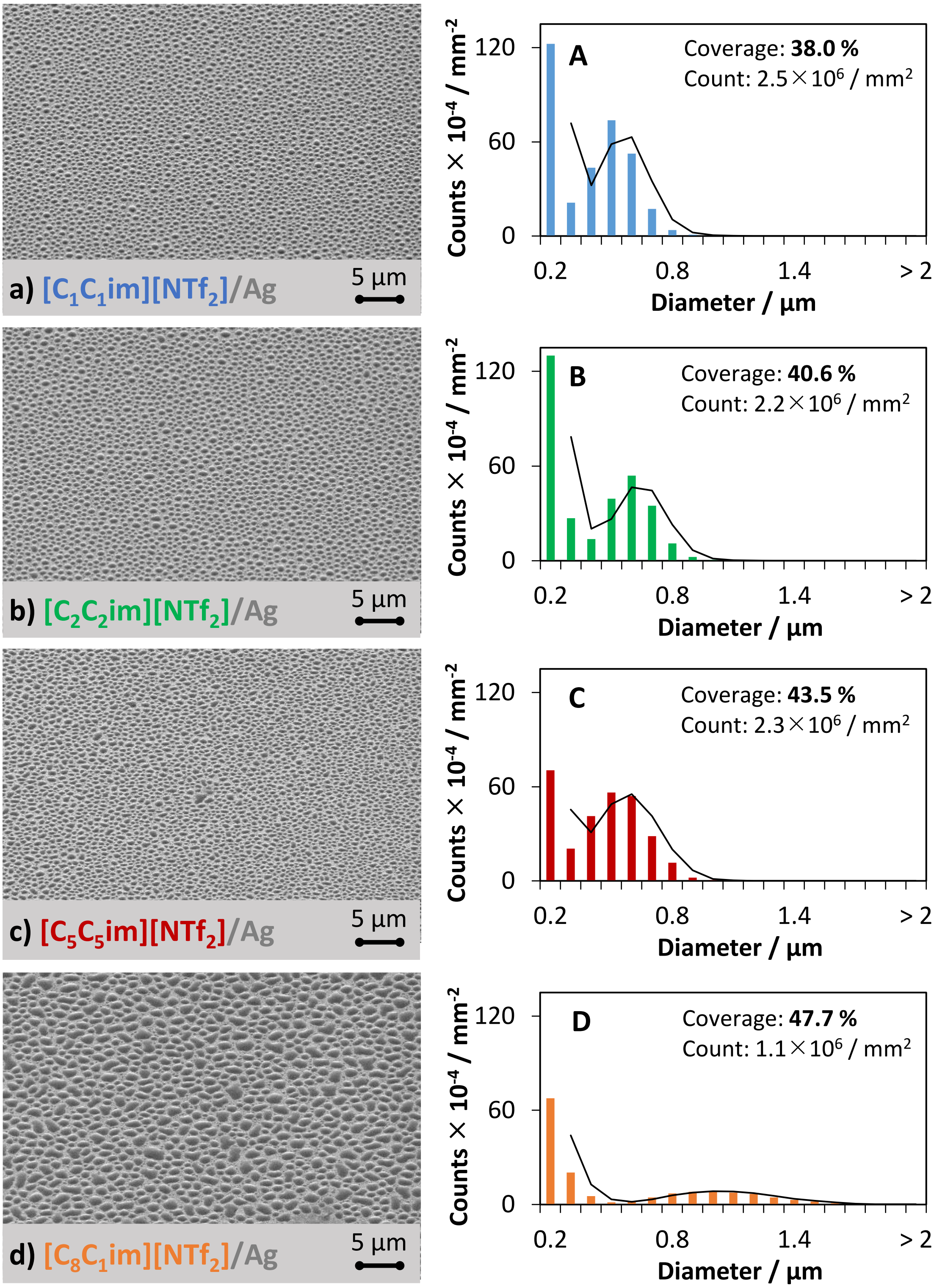

Fig. S7. Morphology of vapor-deposited ionic liquids (50 monolayers) onto silver(Ag)/ITO/glass surfaces (a, b, c, d) and the respective droplet size distribution (A, B, C, D): $[C_1C_1im][NTf_2]$ (a, A), $[C_2C_2im][NTf_2]$ (b, B), $[C_5C_5im][NTf_2]$ (c, C), and $[C_8C_1im][NTf_2]$ (d, D). The ionic liquids were deposited under the same experimental procedure and setup. Micrographs were acquired through high-resolution scanning electron microscopy (SEM) by using a secondary electron detector (SED). Lateral views at 45° were obtained with a magnification of 5000×.

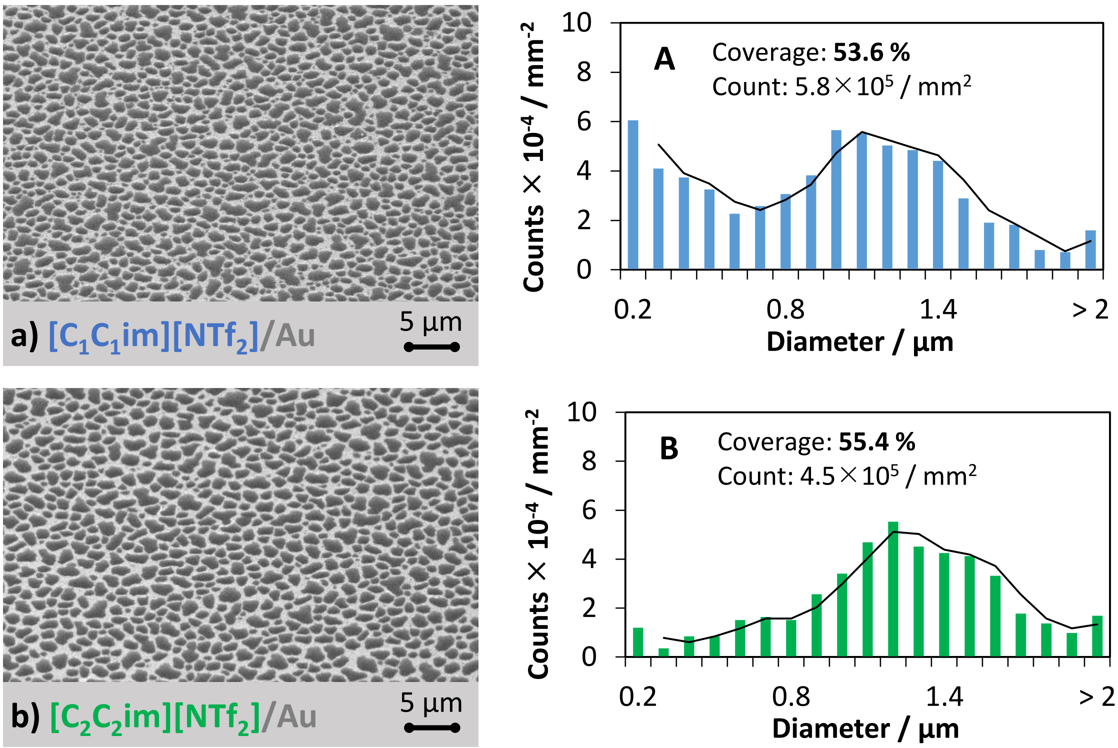

Fig. S8. Morphology of vapor-deposited ionic liquids (50 monolayers) onto gold(Au)/ITO/glass surfaces (a, b) and the respective droplet size distribution (A, B): $[C_1C_1im][NTf_2]$ (a, A) and $[C_2C_2im][NTf_2]$ (b, B). The ionic liquids were deposited under the same experimental procedure and setup. Micrographs were acquired through high-resolution scanning electron microscopy (SEM) by using a secondary electron detector (SED). Lateral views at 45° were obtained with a magnification of 5000×.

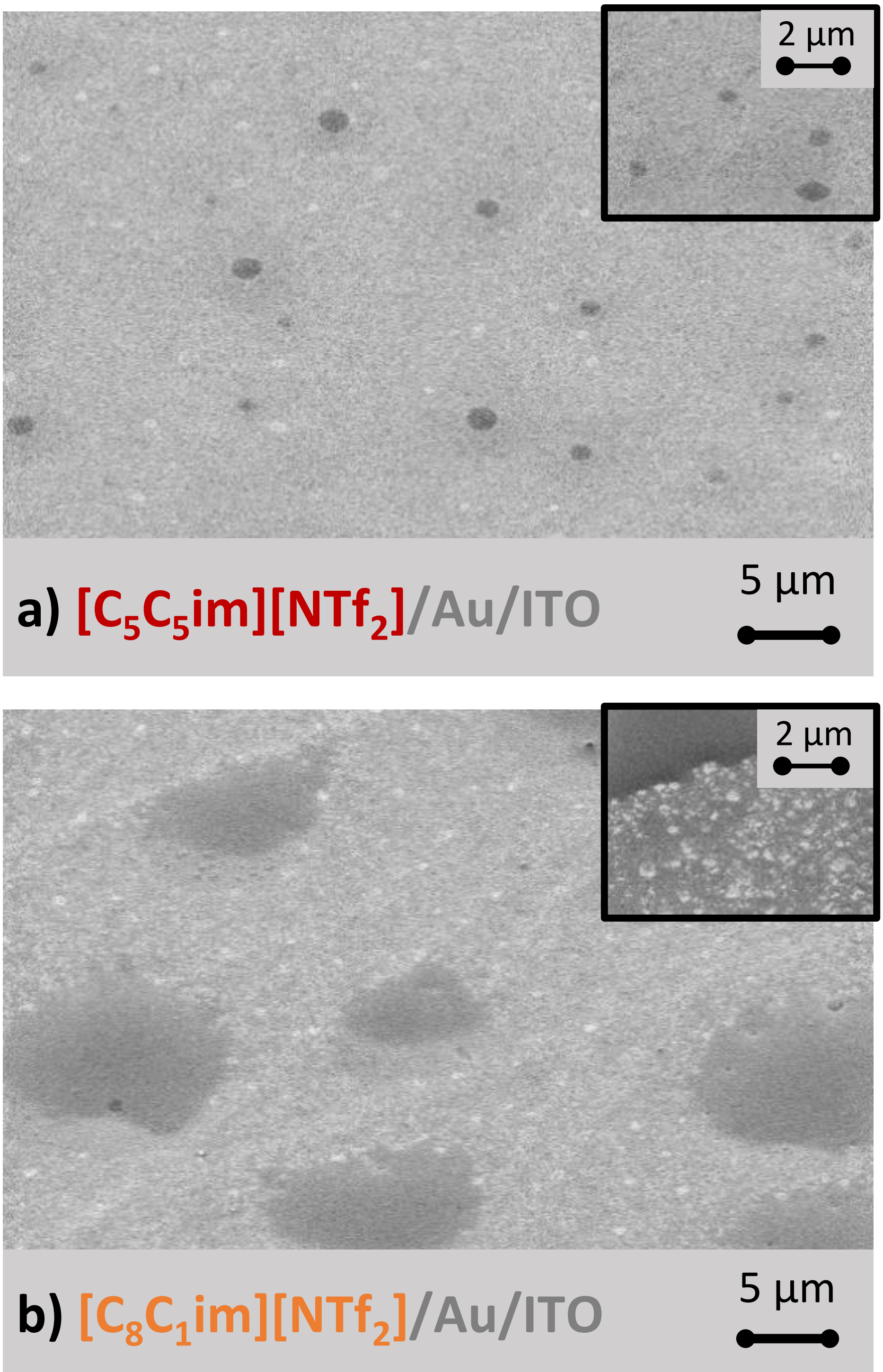

Fig. S9. Detailed Morphology of vapor-deposited ionic liquids (50 monolayers) onto gold(Au)/ITO/glass surfaces (a, b): [C_5C_5im][NTf_2] (a) and [C_8C_1im][NTf_2] (b). The ionic liquids were deposited under the same experimental procedure and setup. Micrographs were acquired through high-resolution scanning electron microscopy (SEM) by using a secondary electron detector (SED). Lateral views at 45° were obtained with a magnification of 5000×.

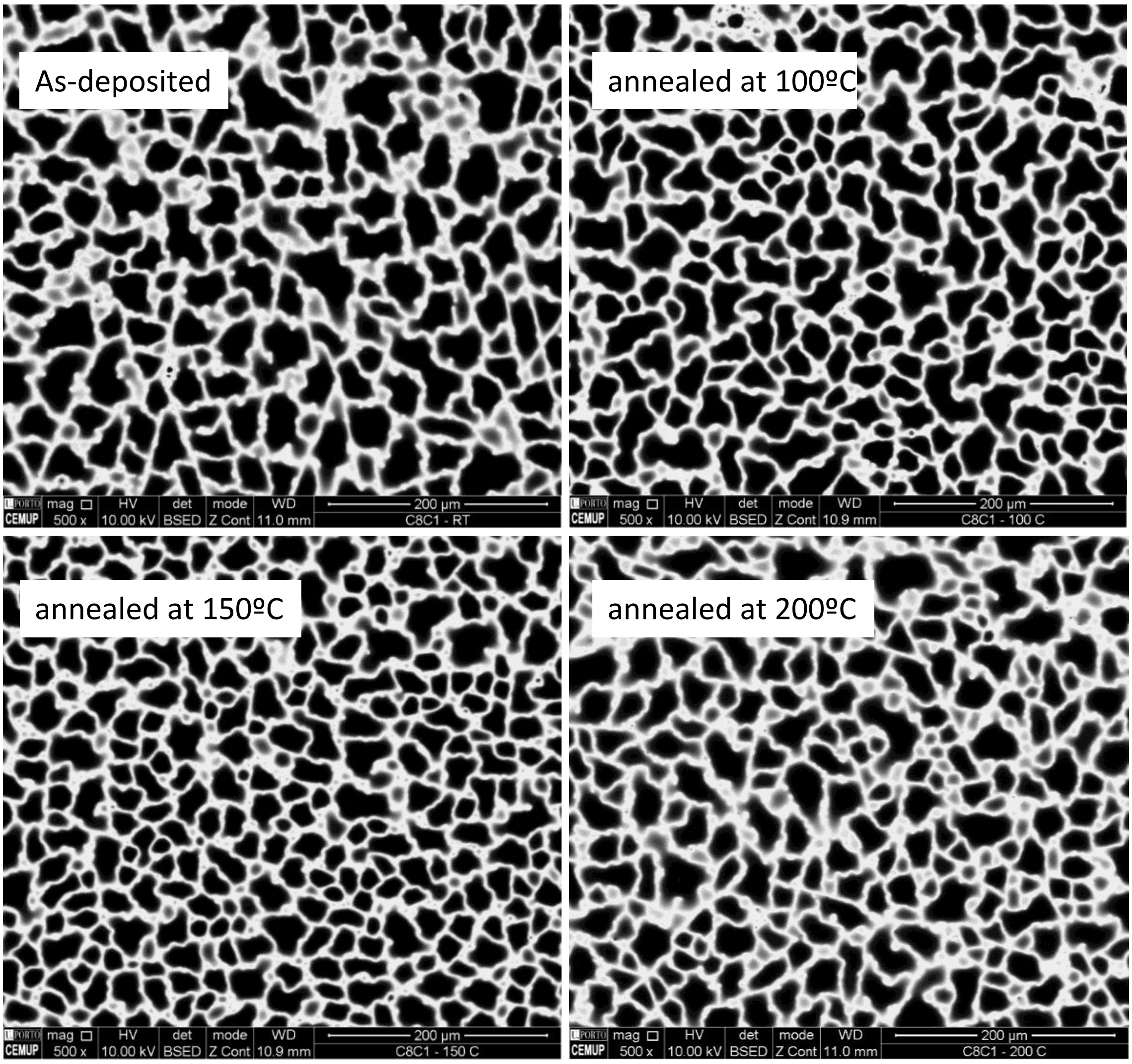

Fig. S10. Morphology of vapor-deposited [C_8C_1im][NTf_2] (400 monolayers) onto gold(Au)/ITO/glass surfaces: as-deposited samples and samples exposed (annealed) to 100ºC, 150ºC, and 200ºC. The impact of the air exposure and heat on the droplet morphology seems to be very reduced.

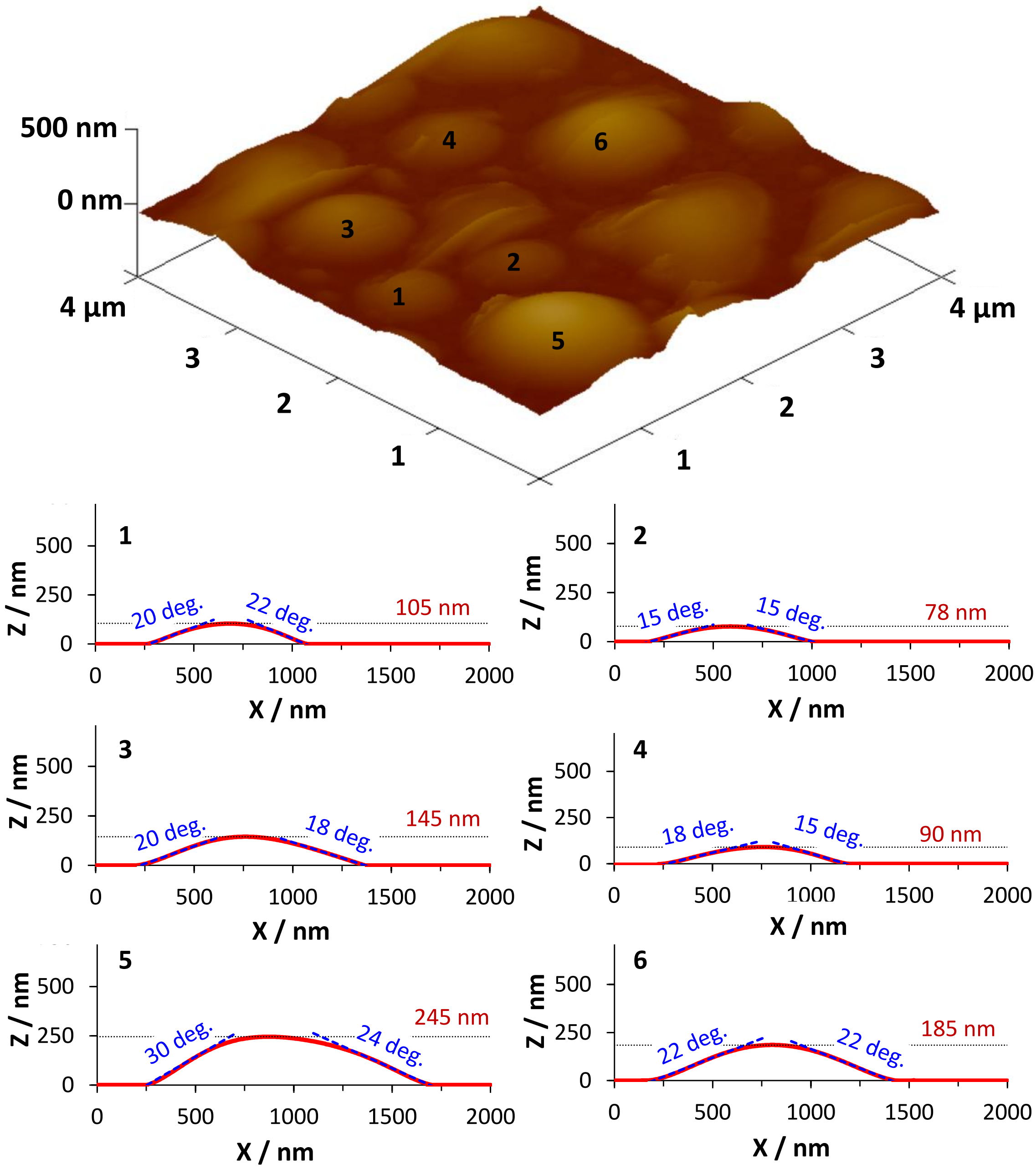

Fig. S11. Three-dimensional AFM image, recorded in a non-contact mode, for vapor-deposited [C_1C_1im][NTf_2] (50 ML) onto the indium tin oxide (ITO)/glass surface. The geometric parameters (dimensions and derived contact angles) of the droplets marked in the AFM image are depicted by graphs 1, 2, 3, 4, 5, and 6.

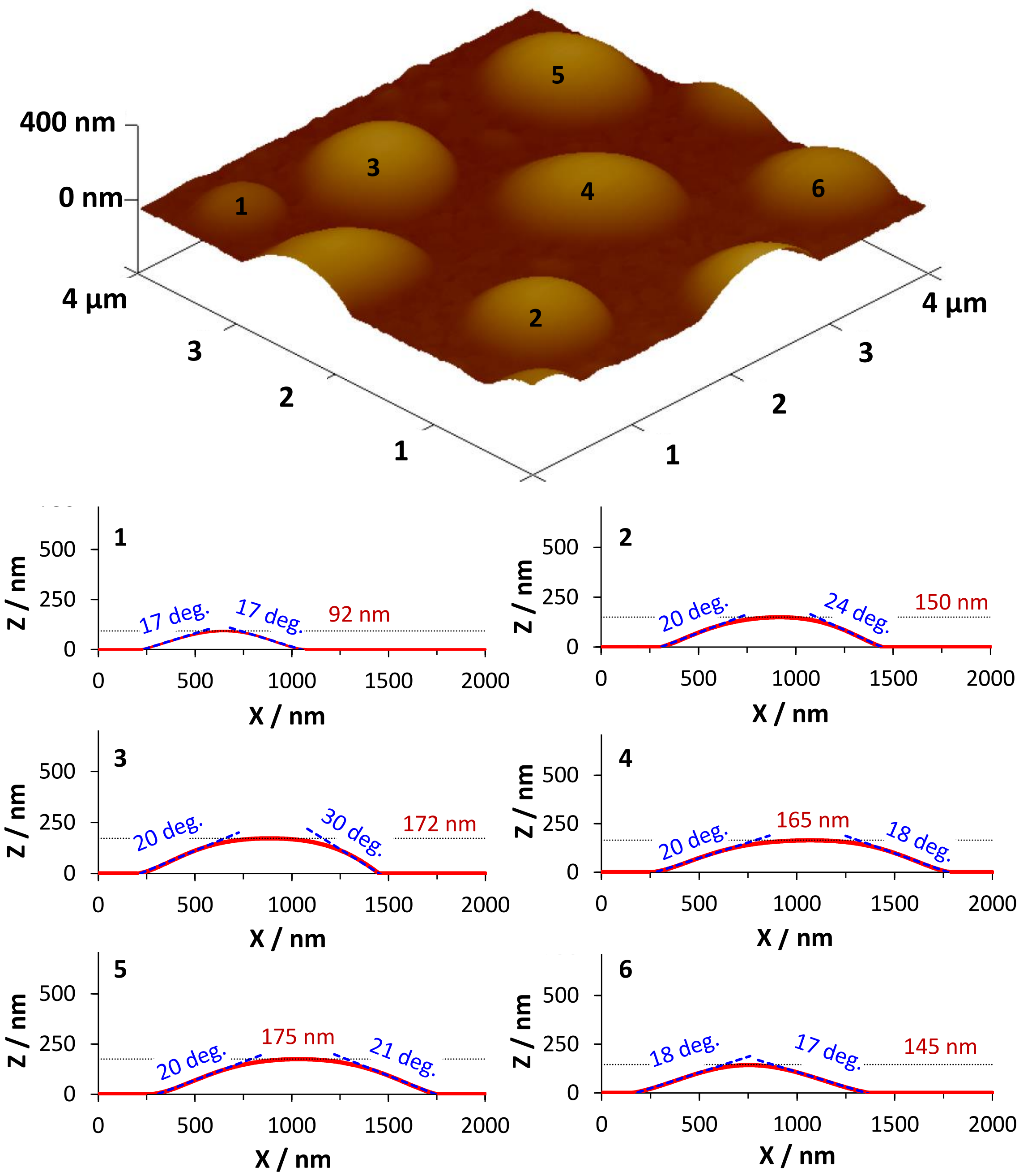

Fig. S12. Three-dimensional AFM image, recorded in a non-contact mode, for vapor-deposited [C_2C_2im][NTf_2] (50 ML) onto the indium tin oxide (ITO)/glass surface. The geometric parameters (dimensions and derived contact angles) of the droplets marked in the AFM image are depicted by graphs 1, 2, 3, 4, 5, and 6.

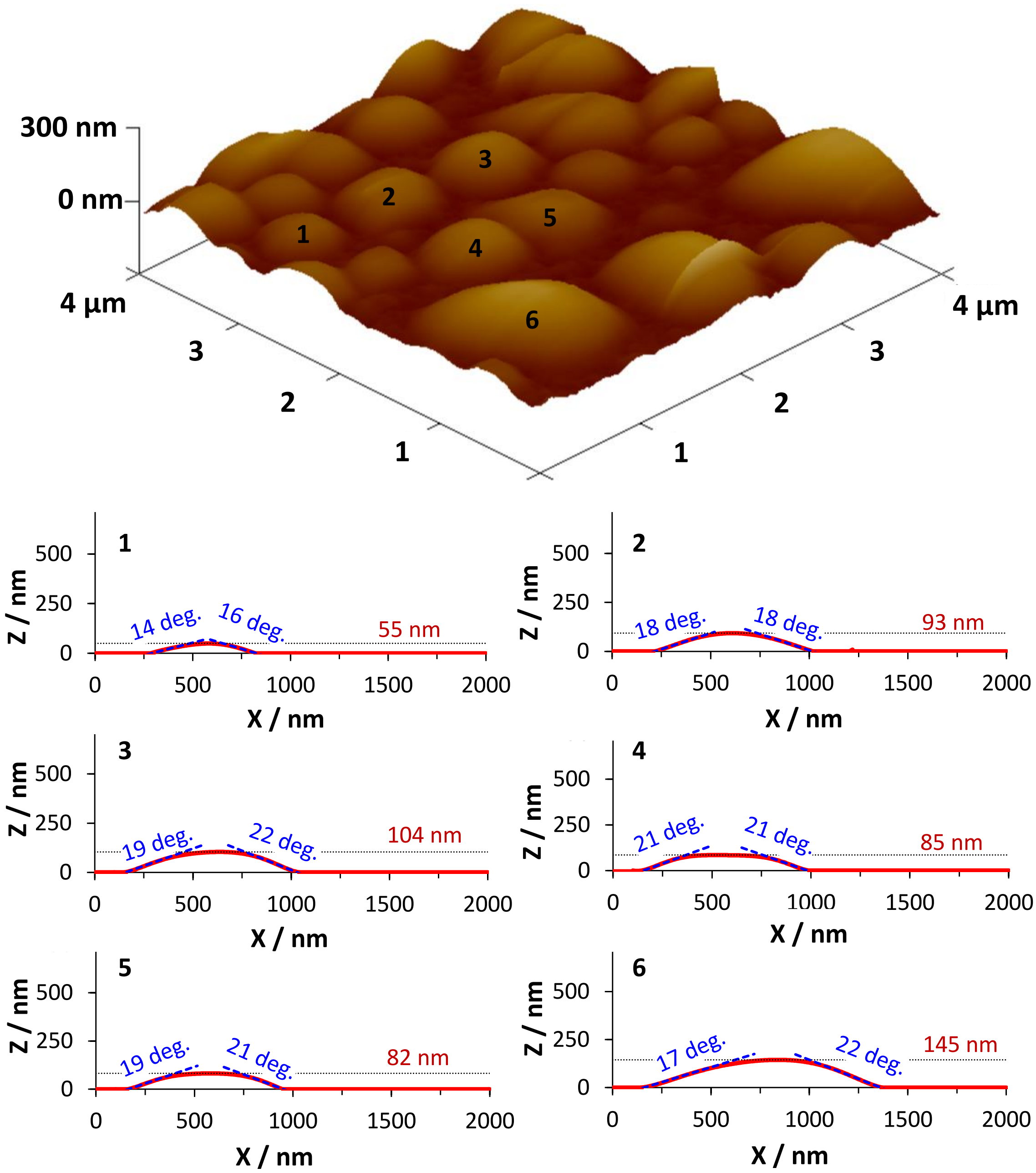

Fig. S13. Three-dimensional AFM image, recorded in a non-contact mode, for vapor-deposited $[C_1C_1im][NTf_2]$ (50 ML) onto the silver(Ag)/ITO/glass surface. The geometric parameters (dimensions and derived contact angles) of the droplets marked in the AFM image are depicted by graphs 1, 2, 3, 4, 5, and 6.

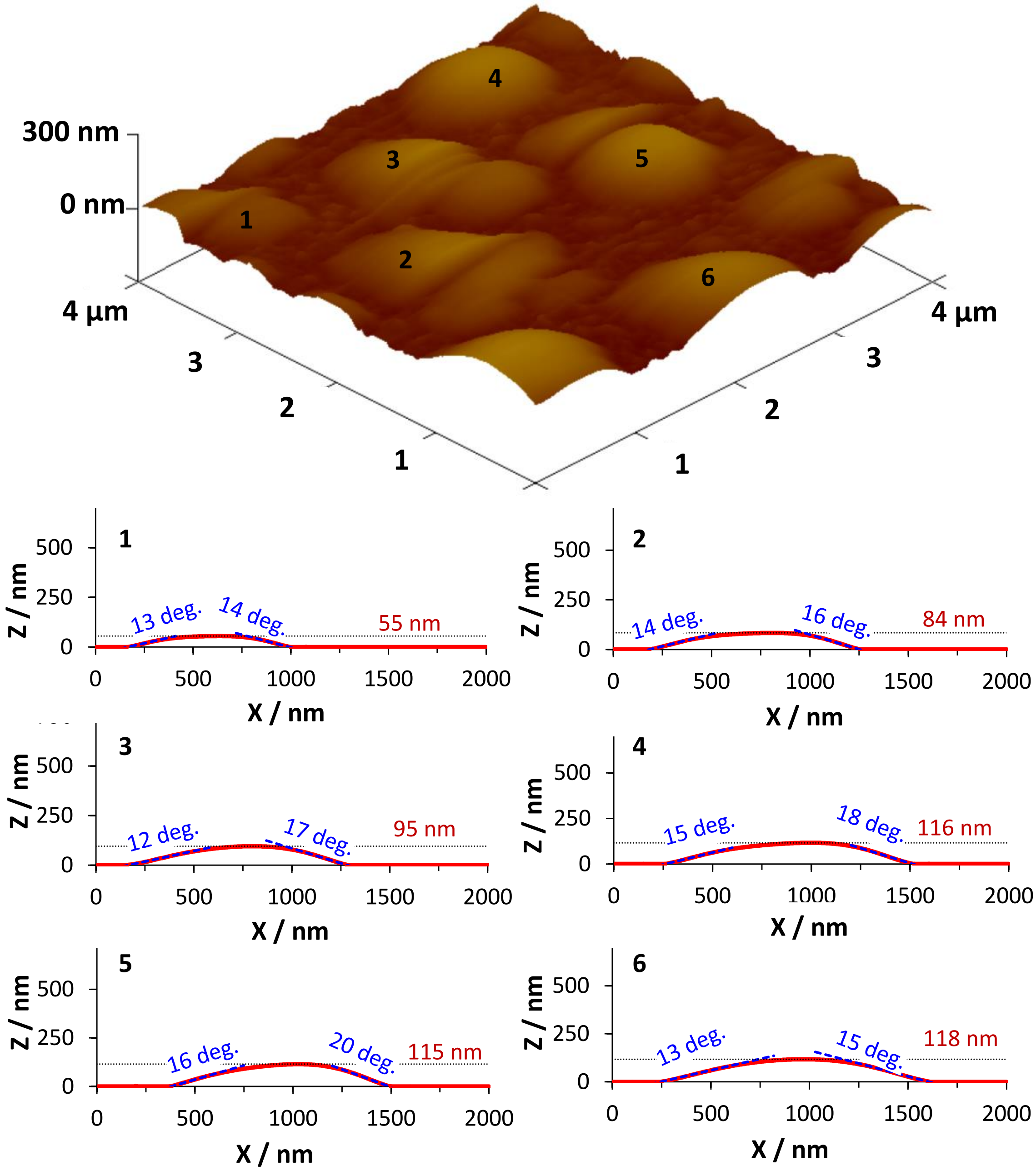

Fig. S14. Three-dimensional AFM image, recorded in a non-contact mode, for vapor-deposited [C_2C_2im][NTf_2] (50 ML) onto the silver(Ag)/ITO/glass surface. The geometric parameters (dimensions and derived contact angles) of the droplets marked in the AFM image are depicted by graphs 1, 2, 3, 4, 5, and 6.

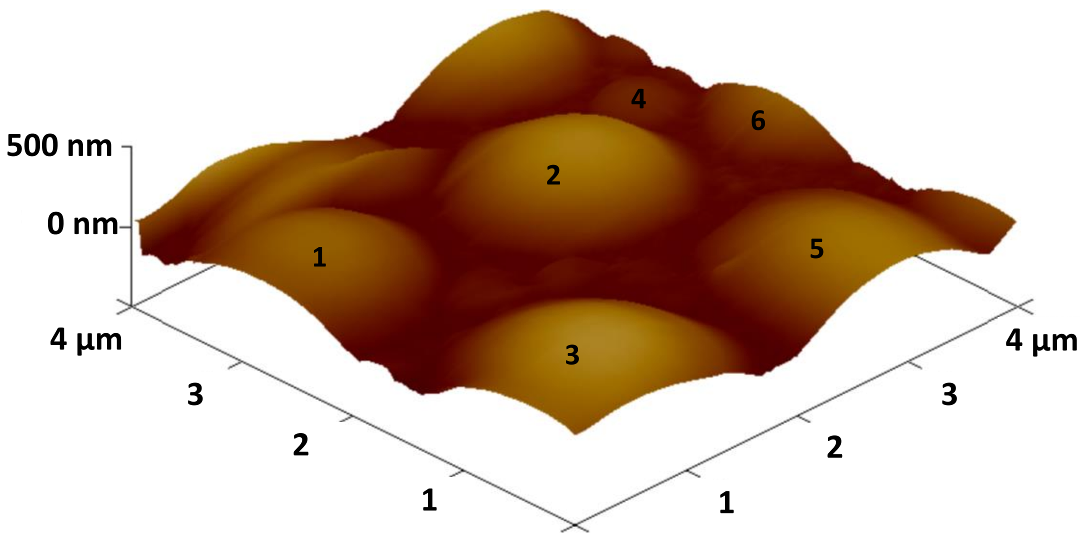

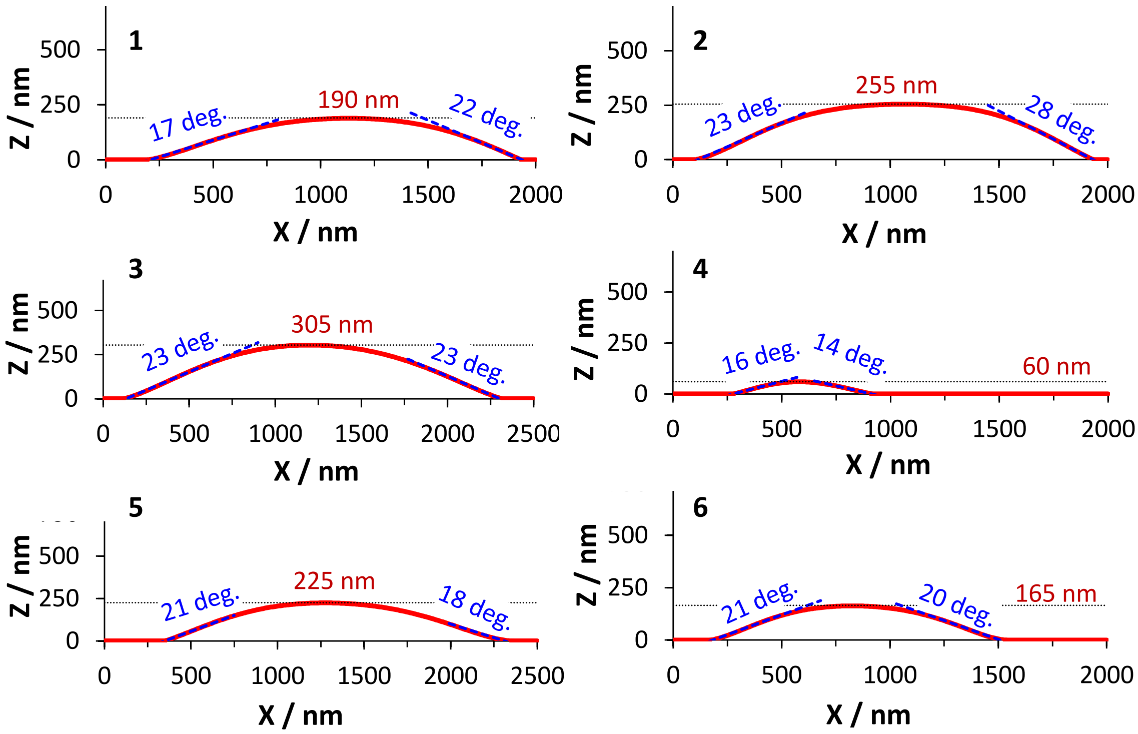

Fig. S15. Three-dimensional AFM image, recorded in a non-contact mode, for vapor-deposited [C_5C_5im][NTf_2] (50 ML) onto the silver(Ag)/ITO/glass surface. The geometric parameters (dimensions and derived contact angles) of the droplets marked in the AFM image are depicted by graphs 1, 2, 3, 4, 5, and 6.

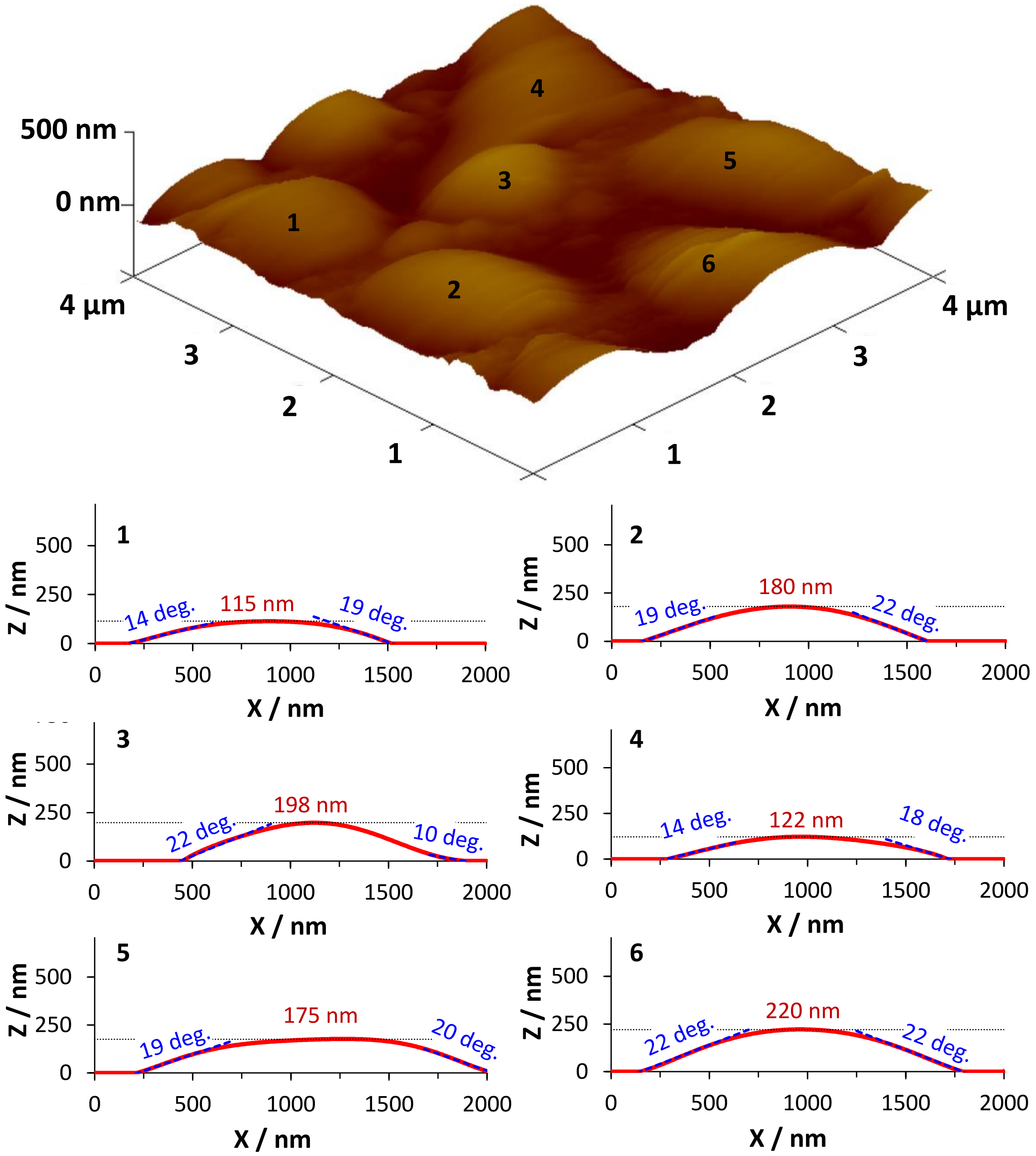

Fig. S16. Three-dimensional AFM image, recorded in a non-contact mode, for vapor-deposited [C_8C_1im][NTf_2] (50 ML) onto the silver(Ag)/ITO/glass surface. The geometric parameters (dimensions and derived contact angles) of the droplets marked in the AFM image are depicted by graphs 1, 2, 3, 4, 5, and 6.

Table S1. Diameter, height, and predicted contact angles (θ) for vapor-deposited micro- and nanodroplets of ionic liquids ($[C_1C_1im][NTf_2]$, $[C_2C_2im][NTf_2]$, $[C_5C_5im][NTf_2]$, and $[C_8C_1im][NTf_2]$) onto ITO and Ag/ITO surfaces.

Ionic liquid	Substrate	Diameter / nm	Height / nm	Diameter / Height	θ/deg.
		840	105	8	20; 22
		820	78	11	15; 15
		1140	145	8	20; 18
$[C_1C_1im][NTf_2]$	ITO	930	90	10	18; 15
		1430	245	6	30; 24
		1230	185	7	22; 22
				8 ± 2	**20 ± 4**
		840	92	9	17; 17
		1130	150	8	20; 24
		1220	172	7	20; 30
$[C_2C_2im][NTf_2]$	ITO	1520	165	9	20; 18
		1430	175	8	20; 21
		1200	145	8	18; 17
				8 ± 1	**20 ± 4**
		520	55	9	14; 16
		810	93	9	18; 18
		880	104	8	19; 22
$[C_1C_1im][NTf_2]$	Ag/ITO	840	85	10	21; 21
		790	82	10	19; 21
		1220	145	8	17; 22
				9 ± 1	**19 ± 3**
		840	55	15	13; 14
		1070	84	13	14; 16
		1120	95	12	12; 17
$[C_2C_2im][NTf_2]$	Ag/ITO	1260	116	11	15; 18
		1120	115	10	16; 20
		1350	118	11	13; 15
				12 ± 2	**15 ± 2**
		1740	190	9	17; 22
		1840	255	7	23; 28
		2200	305	7	23; 23
$[C_5C_5im][NTf_2]$	Ag/ITO	630	60	11	16; 14
		2000	225	9	21; 18
		1360	165	8	21; 20
				9 ± 1	**21 ± 4**
		1350	115	12	14; 19
		1450	180	8	19; 22
		1460	198	7	22; 10
$[C_8C_1im][NTf_2]$	Ag/ITO	1440	122	12	14, 18
		1820	175	10	19, 20
		1650	220	8	22; 22
				9 ± 2	**18 ± 4**

Table S2. Experimental conditions for the physical vapor deposition of various ionic liquids: effusion temperature ($T_{eff.}$); equilibrium vapor pressure (*EVP*); mass flow rate at the Knudsen effusion cell orifice (*Φ* (Knudsen cell)); mass flow rate at the substrate surface (*Φ* (QCM)) and corresponding deposition rate in Å·s^{-1}; geometric factor; deposition time; thin film thickness (nm and ML, ML = monolayers).

Precursor	$T_{eff.}$	*EVP*	*Φ* (Knudsen cell)	*Φ* (QCM)	Geometric factor	Deposition rate	Deposition time	Thickness
	K	Pa	µg·cm^{-2}·s^{-1}	ng·cm^{-2}·s^{-1}		Å·s^{-1}	min	ML
	Ionic Liquid (50 ML) / substrate | substrates: Au/ITO; Ag/ITO; ITO							
[C_1C_1im][NTf_2]	488	≈ 0.09	≈ 31	9.4 ± 3.1	3×10^{-4}	0.6 ± 0.2	10	50
[C_2C_2im][NTf_2]	488	≈ 0.16	≈ 58	7.4 ± 1.5	1×10^{-4}	0.5 ± 0.1	13	
[C_5C_5im][NTf_2]	488	≈ 0.19	≈ 75	7.7 ± 1.3	1×10^{-4}	0.6 ± 0.1	12	
[C_8C_1im][NTf_2]	493	≈ 0.08	≈ 31	6.6 ± 2.6	2×10^{-4}	0.5 ± 0.2	14	
	[C_2C_2im][NTf_2] (200, 400, 600, 800 ML) / ITO-glass							
[C_2C_2im][NTf_2]	488	≈ 0.16	≈ 58	11.8 ± 1.5	2×10^{-4}	0.8 ± 0.1	≈ 32	200
	488			11.8 ± 3.0	2×10^{-4}	0.8 ± 0.2	≈ 64	400
	488			7.4 ± 1.5	1×10^{-4}	0.5 ± 0.1	≈ 154	600
	488			8.9 ± 1.5	2×10^{-4}	0.6 ± 0.1	≈ 171	800
	[C_5C_5im][NTf_2] (200, 400, 600, 800 ML) / ITO-glass							
[C_5C_5im][NTf_2]	488	≈ 0.19	≈ 75	7.7 ± 1.3	1×10^{-4}	0.6 ± 0.1	≈ 48	200
	488			10.3 ± 1.3	1×10^{-4}	0.8 ± 0.1	≈ 71	400
	488			14.2 ± 3.9	2×10^{-4}	1.1 ± 0.3	≈ 78	600
	488			10.3 ± 1.3	1×10^{-4}	0.8 ± 0.1	≈ 152	800